Published in Journal of Reinforced Plastics and Composites (2008)
http://dx.doi.org/10.1177/0731684407085728

A Taguchi Approach for Investigation of Erosion of Glass Fiber – Polyester Composites

AMAR PATNAIK*
Department of Mechanical Engineering
National Institute of Technology, Hamirpur-177005, India
ALOK SATAPATHY AND S. S. MAHAPATRA
Department of Mechanical Engineering National
Institute of Technology, Rourkela 769008, India
R. R. DASH
Department of Mechanical Engineering, G.I.E.T, Gunupur-765022, India

A Taguchi Approach for Investigation of Erosion of Glass Fiber – Polyester Composites

AMAR PATNAIK*
Department of Mechanical Engineering
National Institute of Technology, Hamirpur-177005, India

ALOK SATAPATHY AND S. S. MAHAPATRA
Department of Mechanical Engineering National
Institute of Technology, Rourkela 769008, India

R. R. DASH
Department of Mechanical Engineering, G.I.E.T, Gunupur-765022, India

ABSTRACT: Polyester composites reinforced with three different weight fractions of woven E-glass fiber reinforcement are developed. To study the effect of various operational and material parameters on erosive wear behavior of these composites in an interacting environment, erosion test are carried out. For this purpose, an air jet type erosion test rig and the design of experiments approach utilizing Taguchi's orthogonal arrays are used. The findings of the experiments indicate that erodent size, fiber loading, impingement angle and impact velocity are the significant factors in a declining sequence affecting the wear rate. Significance of erosion efficiency in identifying the wear mechanism is highlighted. It is confirmed that the glass-reinforced-polyester composites exhibit mostly semi-ductile erosion response. An optimal parameter combination is determined, which leads to minimization of erosion rate. Analysis of variance (ANOVA) is performed on the measured data and signal to noise (S/N) ratios. A correlation derived from the results of Taguchi experimental design is proposed as a predictive equation for estimation of erosion wear rate of these composites. It is demonstrated that the predicted results obtained using this equation are consistent with experimental observations. Finally, optimal factor settings for minimum wear rate are determined using genetic algorithm.

KEY WORDS: glass fiber reinforced polyester, taguchi method, design of experiment.

INTRODUCTION

SOLID PARTICLE EROSION is a general term used to describe mechanical degradation (wear) of any material subjected to a stream of erodent particles impinging on its surface. The effect of solid particle erosion has been recognized for a long time [1]. Damage caused by erosion has been reported in several industries for a wide range of situations. Examples can be sited for transportation of airborne solids through pipes [2], boiler tubes exposed to flyash [3] and gas turbine blades [4]. Solid particle erosion is the progressive loss

*Author to whom correspondence should be addressed. E-mail: amar_mech@sify.com

of original material from a solid surface due to mechanical interaction between that surface and solid particles. There have been various reports of applications of polymers and their composites in erosive wear situations in the literature [5–7]. But solid particle erosion of polymers and their composites have not been investigated to the same extent as for metals or ceramics. However, a number of researchers [8,9] have evaluated the resistance of various types of polymers and their composites to solid particle erosion. It is widely recognized that polymers and their composites have poor erosion resistance. Their erosion rates (Ers) are considerably higher than metals. Also, it is well known that the erosion rate of polymer composites is even higher than that of neat polymers [10]. The solid particle erosion behavior of polymer composites as a function of fiber content has been studied to a limited extent [11]. Tilly and Sage [12] have investigated the influence of velocity, impact angle, particle size and weight of impacted abrasives on nylon, carbon-fiber-reinforced nylon, epoxy resin, polypropylene, and glass-fiber-reinforced plastic.

Impact velocity (v) happens to be a critical test variable in erosion, and can easily overshadow changes in other variables, such as target material, impact angle etc. [13]. In addition to velocity, solid particle erosion is governed by the impact angle, particle size, particle shape and hardness [14]. The impact of the above parameters has been studied independently, keeping all parameters at fixed levels. Therefore, visualization of impact of various factors in an interacting environment really becomes difficult. To this end, an attempt has been made to analyse the impact of more than one parameter on solid particle erosion of PMCs, because in actual practice the resultant erosion rate is the combined effect of impact of more than one interacting variable. An inexpensive and easy-to-operate experimental strategy based on Taguchi's parameter design has been adopted to study the effect of various parameters and their interactions. The experimental procedure has been successfully applied for parametric appraisal in the wire electrical discharge machining (WEDM) process, drilling of metal matrix composites, and erosion behavior of metal matrix composites such as aluminum reinforced with red mud [15–21].

The aim of the present study is, therefore, to investigate the erosion behavior of polyester matrix composites based on the Taguchi method under various testing conditions. Furthermore, the analysis of variance is employed to investigate the most significant control factors and their interactions. Finally, an evolutionary approach known as genetic algorithm has been applied for optimal factor settings to minimize the erosion rate.

EXPERIMENTAL DETAILS

Specimen Preparation

Glass fiber reinforced composites are manufactured in the laboratory by the contact molding process. The type of resin used in the present work is polyester (density 1.35 gm/cc) supplied by Ciba-Geigy of India Limited. E-glass fibers (modulus 72.5 GPa and density 2.59 gm/cc) supplied by Saint Govion Ltd. is employed as the reinforcing phase. The cross-plied fiber sheets are reinforced in the polyester. Composite slabs of three different compositions (i.e. fiber content of 30, 40, and 50 wt%) are made. The castings are cured at room temperature for about 24 h. Specimens of suitable dimension were cut using a diamond cutter for further characterization and erosion tests.

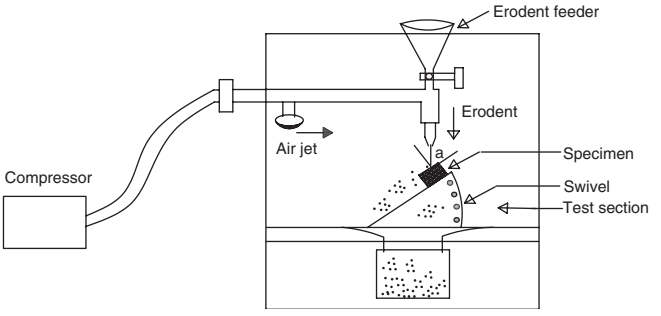

Figure 1. *A schematic diagram of the erosion rig.*

Table 1. Levels of the variables used in the experiment.

	Level			
Control factor	**I**	**II**	**III**	**Units**
A: Velocity of impact	32	45	58	m/sec
B: Fiber loading	30	40	50	%
C: Stand-off distance	120	180	240	Mm
D: Impingement angle	30	60	90	Degree
E: Erodent size	300	500	800	μm

Test Apparatus

The room temperature erosion test facility used in the present investigation is illustrated schematically in Figure 1. The set up is capable of creating a reproducible erosive situation for assessing erosion wear resistance of the prepared composite samples. The conditions (confirming to ASTM G 76 test standards) under which erosion tests are carried out are listed in Table 1. Dry silica sand (density 2.5 gm/cc) is used as the erodent. The particles fed at a constant rate are made to flow with compressed air jet to impact the specimen, which can be held at various angles with respect to the flow direction of erodent using a swivel and an adjustable sample clip. The velocity of the eroding particles is determined using the double disc method (Aglan and Chenock [7]). The samples were cleaned in acetone, dried and weighed to an accuracy of ± 0.1 mg accuracy using a precision electronic balance. These are then eroded in the test rig for 10 min and weighed again to determine the weight loss. The procedure is repeated till the erosion rate attains a constant value called the steady state erosion rate. The ratio of this weight loss to the weight of the eroding particles causing the loss (i.e. testing time $\times$ particle feed rate) is then computed as the dimensionless incremental erosion rate.

Experimental Design

Design of experiment is a powerful analysis tool for modeling and analysing the influence of control factors on performance output. The most important stage in the design of experiment lies in the selection of the control factors. Therefore, a large number of factors are included so that non-significant variables can be identified at the earliest opportunity. The operating conditions under which erosion tests were carried out are given in Table 1. The tests were conducted as per experimental design given in Table 2 at room temperature.

Table 2. Orthogonal array for L_{27} (3^{13}) Taguchi design.

$L_{27}(3^{13})$	1 A	2 B	3 $(A \times B)_1$	4 $(A \times B)_2$	5 C	6 $(B \times C)_1$	7 $(B \times C)_2$	8 $(A \times C)_1$	9 D	10 E	11 $(A \times C)_2$	12	13
1	1	1	1	1	1	1	1	1	1	1	1	1	1
2	1	1	1	1	2	2	2	2	2	2	2	2	2
3	1	1	1	1	3	3	3	3	3	3	3	3	3
4	1	2	2	2	1	1	1	2	2	2	3	3	3
5	1	2	2	2	2	2	2	3	3	3	1	1	1
6	1	2	2	2	3	3	3	1	1	1	2	2	2
7	1	3	3	3	1	1	1	3	3	3	2	2	2
8	1	3	3	3	2	2	2	1	1	1	3	3	3
9	1	3	3	3	3	3	3	2	2	2	1	1	1
10	2	1	2	3	1	2	3	1	2	3	1	2	3
11	2	1	2	3	2	3	1	2	3	1	2	3	1
12	2	1	2	3	3	1	2	3	1	2	3	1	2
13	2	2	3	1	1	2	3	2	3	1	3	1	2
14	2	2	3	1	2	3	1	3	1	2	1	2	3
15	2	2	3	1	3	1	2	1	2	3	2	3	1
16	2	3	1	2	1	2	3	3	1	2	2	3	1
17	2	3	1	2	2	3	1	1	2	3	3	1	2
18	2	3	1	2	3	1	2	2	3	1	1	2	3
19	3	1	3	2	1	3	2	1	3	2	1	3	2
20	3	1	3	2	2	1	3	2	1	3	2	1	3
21	3	1	3	2	3	2	1	3	2	1	3	2	1
22	3	2	1	3	1	3	2	2	1	3	3	2	1
23	3	2	1	3	2	1	3	3	2	1	1	3	2
24	3	2	1	3	3	2	1	1	3	2	2	1	3
25	3	3	2	1	1	3	2	3	2	1	2	1	3
26	3	3	2	1	2	1	3	1	3	2	3	2	1
27	3	3	2	1	3	2	1	2	1	3	1	3	2

Five parameters, viz., impact velocity, fiber loading, stand-off distance, impingement angle, and erodent size, each at three levels, are considered in this study in accordance with L_{27} (3^{13}) orthogonal array design. In Table 2, each column represents a test parameter and a row gives a test condition which is nothing but a combination of parameter levels. Five parameters each at three levels would require $3^5 = 243$ runs in a full factorial experiment. Whereas Taguchi's factorial experiment approach reduces it to only 27 runs, offering a great advantage.

The experimental observations are transformed into a signal-to-noise (S/N) ratio. There are several S/N ratios available depending on the type of characteristics. The S/N ratio for minimum erosion rate coming under smaller is better characteristic, which can be calculated as logarithmic transformation of the loss function as shown below.

Smaller is the better characteristic:

$$\frac{S}{N} = -10 \log \frac{1}{n} \left(\sum y^2 \right) \tag{1}$$

where n the number of observations, and y the observed data. The "lower is better" (LB) characteristic, with the above S/N ratio transformation, is suitable for minimizations of erosion rate. The standard linear graph, as shown in Figure 2, is used to assign the factors and interactions to various columns of the orthogonal array [22,23]. Solid particle erosion is characterized by a large number of factors such as impact velocity, fiber loading, stand

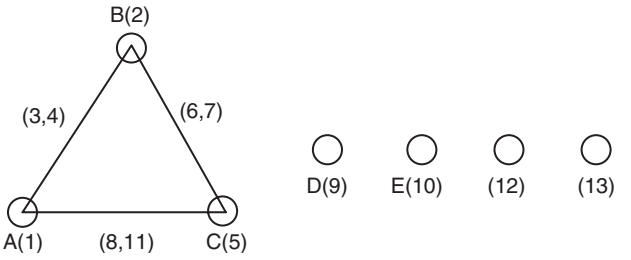

Figure 2. *Standard linear graphs for L_{27} array.*

off-distance, impingement angle, and erodent size. Out of all these factors, velocity predominantly governs the rate of erosion.

The plan of the experiments is as follows: the first column was assigned to impact velocity (A), the second column to fiber loading (B), the fifth column to stand-off distance (C), the ninth column to impingement angle (D) and tenth column to erodent size (E), the third and fourth column are assigned to $(A \times B)_1$ and $(A \times B)_2$, respectively, to estimate interaction between impact velocity (A) and fiber loading (B), the sixth and seventh column are assigned to $(B \times C)_1$ and $(B \times C)_2$, respectively, to estimate interaction between the fiber loading (B) and stand-off distance (C), the eighth and eleventh column are assigned to $(A \times C)_1$ and $(A \times C)_2$, respectively, to estimate interaction between the impact velocity (A) and stand-off distance (C). The remaining columns are assigned to error columns, respectively.

RESULTS AND DISCUSSION

Steady State Erosion

Erosion wear behavior of materials can be grouped as ductile and brittle categories although this grouping is not definitive. Thermoplastic matrix composites usually show ductile behavior and have the peak erosion rate at around 30° impact angle because the cutting mechanism is dominant in erosion, the thermosetting ones erode in a brittle manner with the peak erosion occurring at normal impact. However, there is a dispute about this failure classification as the erosive wear behavior depends strongly on the experimental conditions and the composition of the target material [8]. Figure 3 shows the impact angle dependence of the erosion rate of polyester composites with different fiber content. The erosion curves are plotted from the results of erosion tests conducted for different impingement angle keeping all other parameters constant (impact velocity = 32 m/sec, stand-off distance = 120 mm and erodent size = 300 μm). It can be seen that the peaks of erosion rates are located at an angle of 60° for all the samples irrespective of fiber content. This shows semi-ductile erosion behavior of the composite. It is further noted in Figure 3 that with increased fiber content the erosion rate of the composites is greater. This can be attributed to the fact that the harder the material, the larger is the fraction of the crater volume that is removed [24]. In this investigation, higher hardness values have been noted for composites with higher fiber loading and this is one reason why the composites exhibit declining erosion resistance with the increase in fiber content.

To identify the mode of material removal, the morphologies of eroded surfaces are observed under a scanning electron microscope. Figure 4 presents the microstructure of

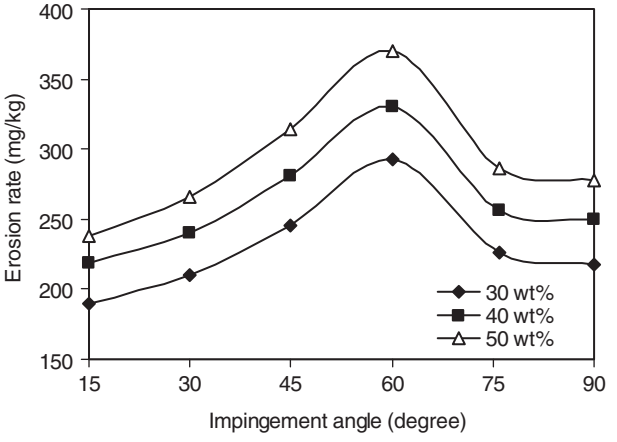

Figure 3. *Erosion rate vs. angle of impingement for different fiber loading.*

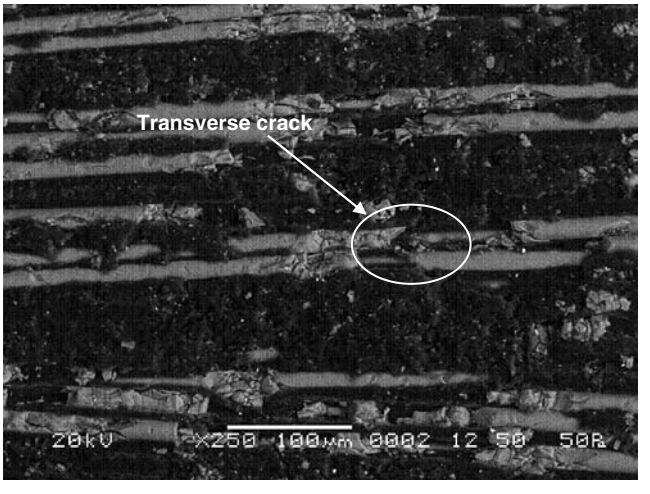

Figure 4. *SEM micrograph (X 250) of GF Polymer composite eroded surface (impact velocity 58 m/sec, fiber loading 50%, S.O.D 120 mm, impingement angle 60° and erodent size 300 μm).*

the composite eroded at high impact velocity (58 m/sec), at lower stand-off distance (120 mm) and at an impingement angle of 60°. It shows local removal of resin material from the impacted surface resulting in exposure of the fibers to the erodent flux. This micrograph also reveals that, due to sand particle impact on fibers, there is formation of transverse cracks that break these fibers. Figure 5 presents the magnified microstructure of the composite eroded at the same conditions. Here the propagation of crack along transverse as well as longitudinal direction is well visualized. On comparing this microstructure with that of the same composite eroded at a lower impact velocity (45 m/s), higher stand-off distance (240 mm) and higher impingement angle (90°), it can be seen that in the second case, the breaking of glass fibers is more prominent (Figure 6). It appears that cracks have grown on the fibers giving rise to breaking of the fibers into

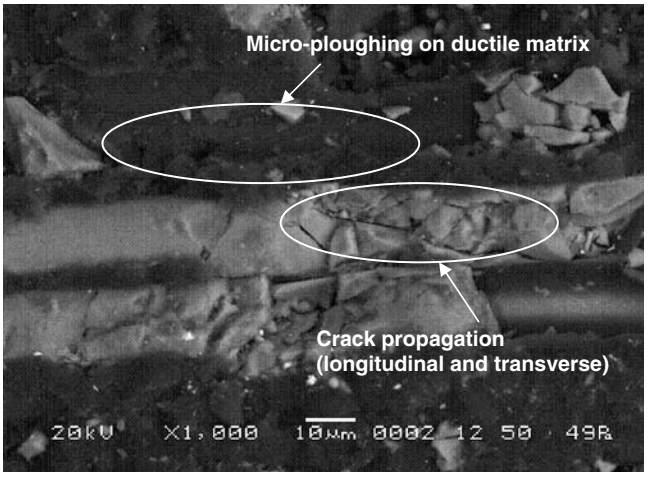

Figure 5. *SEM micrograph (X 1000) of GF Polymer composite eroded surface (impact velocity 58 m/sec, fiber loading 50%, S.O.D 120 mm, impingement angle 60° and erodent size 300 μm).*

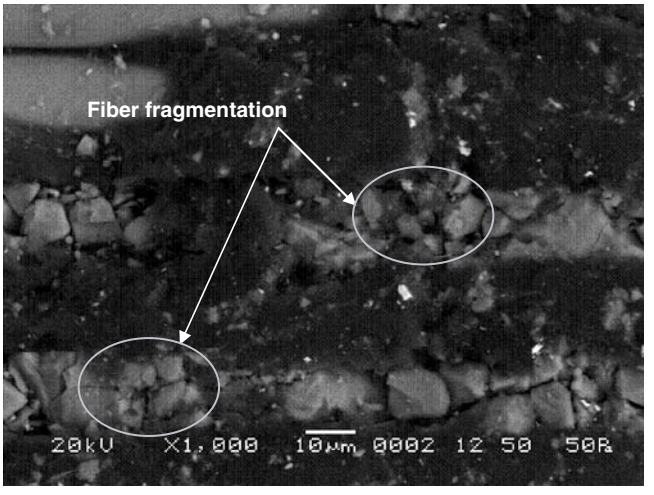

Figure 6. *SEM micrograph (X 1000) of GF Polymer composite eroded surface (impact velocity 45 m/sec, fiber loading 50%, S.O.D 240 mm, impingement angle 90° and erodent size 800 μm).*

small fragments. Further the cracks have been annihilated at the fiber matrix interface and seem not to have penetrated through the matrix. Change in impact angle from oblique to normal changes the topography of the damaged surface very significantly. Figure 6 shows the dominance of micro-chipping and micro-cracking phenomena. It can be seen that multiple cracks originate from the point of impact, intersect one another and form wear debris due to brittle fracture in the fiber body. After repetitive impacts, the debris in platelet form are removed and account for the measured wear loss. The occurrence of peak erosion rate at 60° impact is understandable. In this case, both abrasion and erosion processes play important roles. After impacting, the sand particles, slide on the surface and

abrade while dropping down. The wear and subsequently the damage are therefore more than that in the case of normal impact. Marks of micro-ploughing on the ductile polyester matrix region seen in Figure 5 support this argument.

Polyester is a thermoplastic polymer and it is known that it shows ductile erosion response. So a possible reason for the semi-ductile erosion behavior exhibited by the polyester based composites in the present investigation is that the glass fibers used as reinforcements for polyester matrix are a typical brittle material. Their erosion is caused mostly by damage mechanism such as micro-cracking. Such damage is supposed to increase with the increase of kinetic energy loss of the impinging sand particles. According to Hutchings et al. [25], kinetic energy loss is maximum at normal impact, where erosion rates are highest for brittle materials. In the present study, the peak erosion rate shifts to a larger value of impingement angle (60°), which is clearly due to the brittle nature of glass fibers. So, although polyester is a ductile material, the presence of fibers makes the composite relatively more sensitive to impact energy which increases when the impact mode pattern changes from tangential ($\alpha = 0°$) to normal ($\alpha = 90°$). This explains the semi-ductile nature of the glass-polyester composites with respect to solid particle erosion.

From Table 3, the overall mean for the S/N ratio of the erosion rate is found to be −48.97 db. Figure 7 shows graphically the effect of the six control factors on erosion rate. The analysis was made using the popular software, specifically used for design of experiment applications, known as MINITAB 14. Before any attempt is made to use this simple model as a predictor for the measures of performance, the possible interactions between the control factors must be considered. Thus factorial design incorporates a simple means of testing for the presence of the interaction effects.

Analysis of the result leads to the conclusion that factor combination of A_1, B_2, C_1, D_1, and E_2 gives minimum erosion rate. The interaction graphs are shown in Figures 8–10. As far as minimization of erosion rate is concerned, factors B and E have significant effects whereas factor C has least effect. It is observed from Figure 8 that the interaction between A × B shows most significant effect on erosion rate. But the factor C individually has less contribution on output performance, and their combination of interaction with factor A and B (A × C and B × C), shown in Figures 9 and 10 can be neglected for further study.

A similar observation is made in the surface plots of erosion rate with significant control factors (Figures 11a–c). From this analysis, it is concluded that, among all the factors, stand-off distance is most insignificant while impact velocity has relatively less significance compared to the other remaining factors. Figure 11a shows the significant interaction between impact velocity and fiber loading for minimization of erosion rate. The main effects plot for S/N ratio for erosion rate indicates the selection of medium fiber loading (40%), lower impact velocity (32 m/sec) and lower stand-off distance (120 mm) results in the best combination to get minimum erosion rate, within the selected range of experiment. Using Figure 7 for S/N ratio, the optimum combination of significant control factors is A_1, B_2, and C_1. Surface response plot Figure 12 indicates that minimum erosion rate can be achieved in composite with medium fiber loading eroded at a smaller impact velocity region.

Erosion Efficiency

The hardness alone is unable to provide sufficient correlation with erosion rate, largely because it determines only the volume displaced by each impact and not really the volume eroded. Thus a parameter which will reflect the efficiency with which the displaced volume

Table 3. Experimental design using L_{27} orthogonal array.

Sl. No	Impact velocity (A) (m/sec)	Fiber loading (B) (%)	Stand-off distance (C) (mm)	Impingement angle (D) (Degree)	Erodent size (E) (μm)	Erosion rate (Er) (mg/kg)	S/N ratio (db)
1	32	30	120	30	300	309.83	−49.8225
2	32	30	180	60	500	315.25	−49.9731
3	32	30	240	90	800	305.19	−49.6914
4	32	40	120	60	500	186.07	−45.3936
5	32	40	180	90	800	272.79	−48.7166
6	32	40	240	30	300	230.96	−47.2707
7	32	50	120	90	800	287.69	−49.1785
8	32	50	180	30	300	279.85	−48.9385
9	32	50	240	60	500	255.25	−48.1393
10	45	30	120	60	800	288.86	−49.2137
11	45	30	180	90	300	249.80	−47.9518
12	45	30	240	30	500	255.25	−48.1393
13	45	40	120	90	300	239.76	−47.5955
14	45	40	180	30	500	249.18	−47.9304
15	45	40	240	60	800	298.23	−49.4910
16	45	50	120	30	500	261.17	−48.3385
17	45	50	180	60	800	364.31	−51.2294
18	45	50	240	90	300	389.94	−51.8201
19	58	30	120	90	500	315.10	−49.9690
20	58	30	180	30	800	245.19	−47.7901
21	58	30	240	60	300	219.89	−46.8441
22	58	40	120	30	800	261.27	−48.3418
23	58	40	180	60	300	239.76	−47.5955
24	58	40	240	90	500	210.66	−46.4716
25	58	50	120	60	300	369.47	−51.3516
26	58	50	180	90	500	452.81	−53.1183
27	58	50	240	30	800	391.45	−51.8535

is removed should be combined with hardness to obtain a better correlation. The erosion efficiency is obviously one such parameter. In the case of a stream of particles impacting a surface normally (i.e. at $\alpha = 90^{\circ}$), erosion efficiency (η_{normal}) defined by Sundararajan et al. [14] is given as

$$\eta_{\text{normal}} = \frac{2ErHv}{\rho V^2} \tag{2a}$$

but considering impact of erodent at any angle α to the surface, the actual erosion efficiency (η) can be obtained by modifying equation (2a) as

$$\eta = \frac{2ErHv}{\rho V^2 \text{Sin}^2\alpha} \tag{2b}$$

where E_r the erosion rate (kg/kg), H_v the hardness of target material (Pa), ρ the density of the erodent (kg/m^3) and V the impact velocity (m/sec).

The values of erosion efficiencies of these composites calculated using equation (2b) are summarized in Table 4 along with their hardness values and operating conditions.

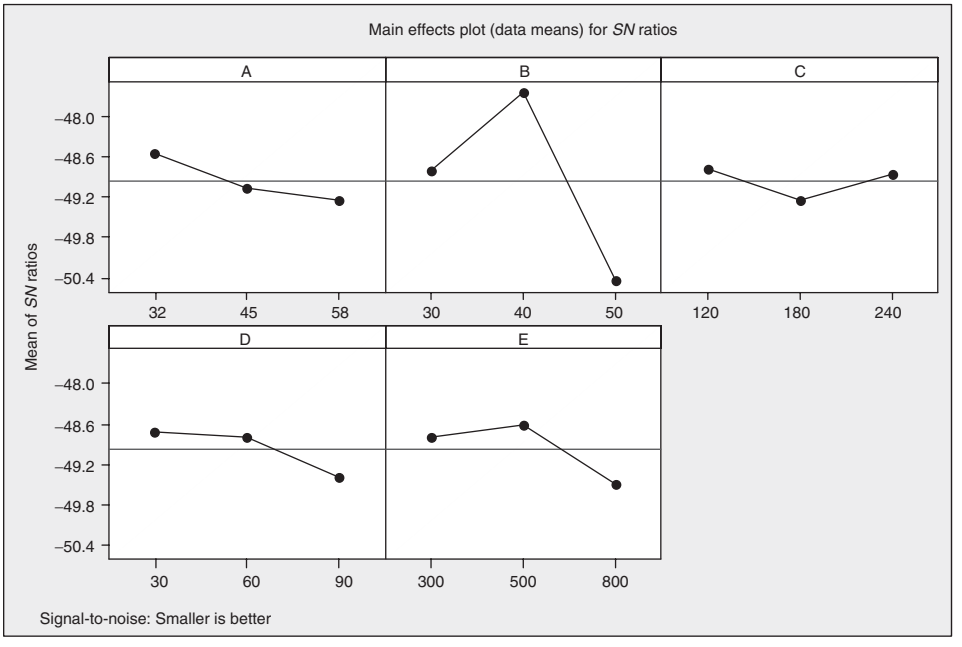

Figure 7. *Effect of control factors on erosion rate.*

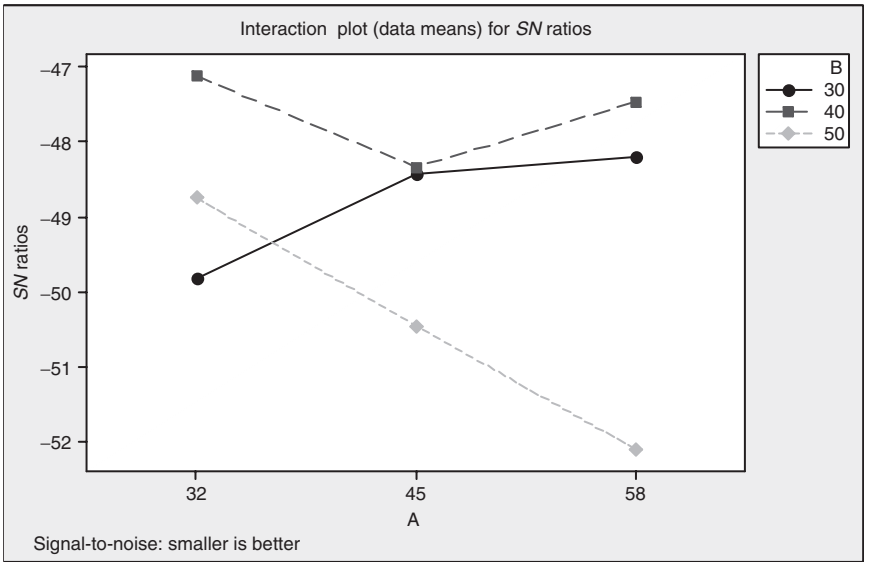

Figure 8. *Interaction graph between A × B for erosion rate.*

It clearly shows that erosion efficiency is not exclusively a material property, but also depends on other operational variables such as impingement angle and impact velocity. The erosion efficiencies of these composites under normal impact (η_{normal}) vary from 3–6, 6–9, and 9–12% for impact velocities 58, 45 and 32 m/sec, respectively.

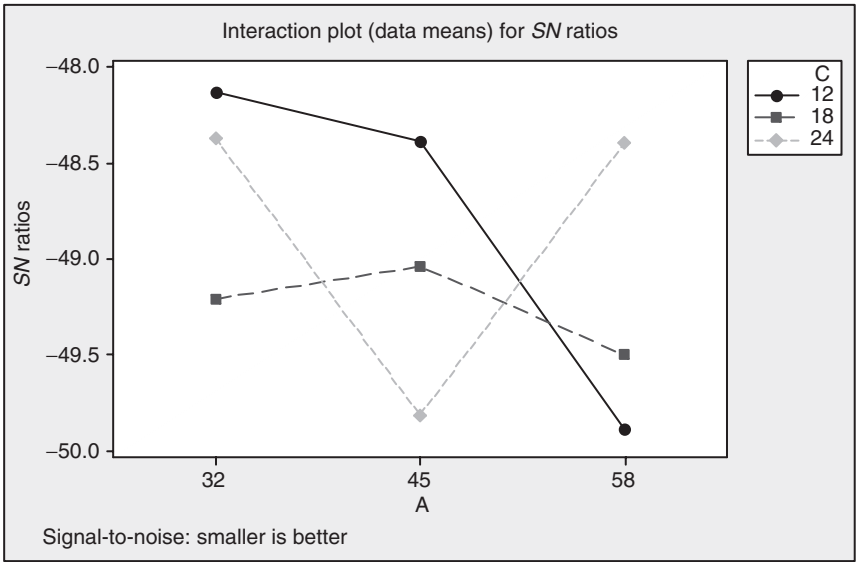

Figure 9. *Interaction graph between A × C for erosion rate.*

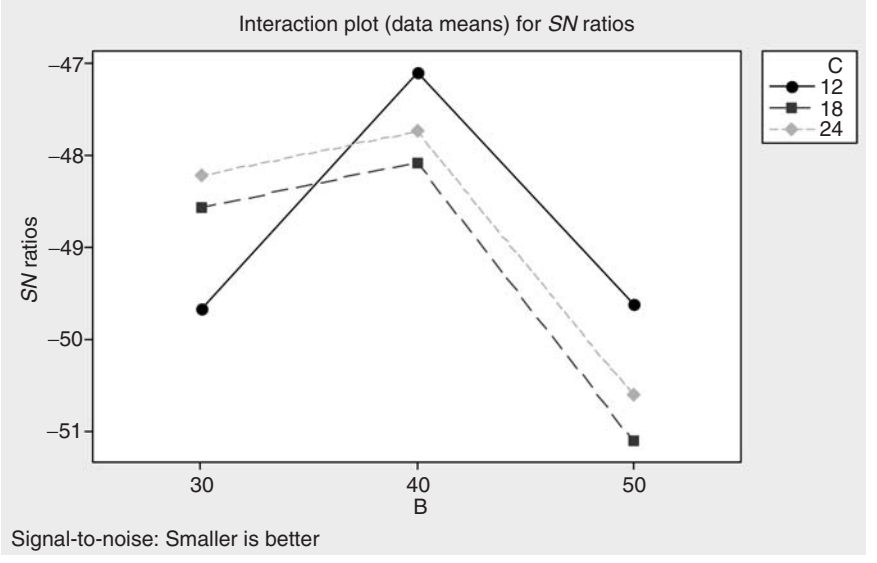

Figure 10. *Interaction graph between B × C for erosion rate.*

The value of η for a particular impact velocity under oblique impact can be obtained simply by multiplying a factor $1/\mathrm{Sin}^2\alpha$ with $\eta_{\mathrm{normal.}}$ Similar observations on velocity dependence of erosion efficiency have previously been reported by few investigators [26,27].

The magnitude of η can be used to characterize the nature and mechanism of erosion. For example, ideal microploughing involving just the displacement of the material from

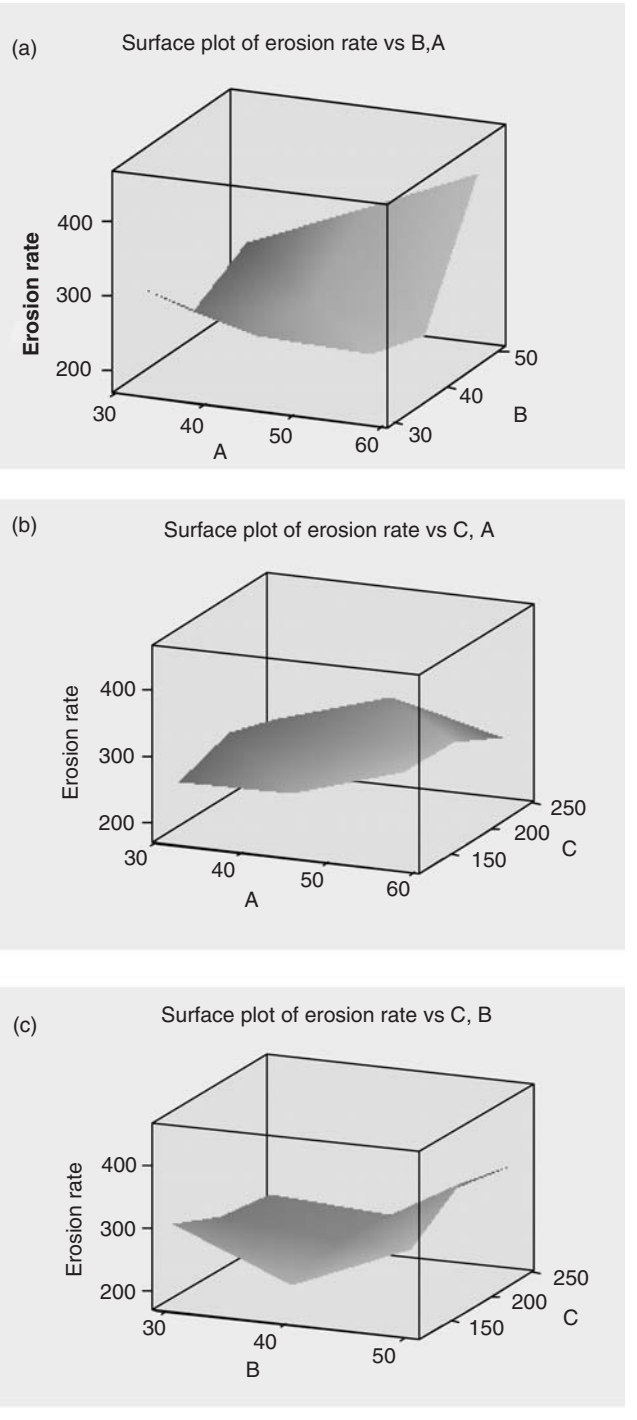

Figure 11. *(a) Surface plot of erosion rate vs. A × B interaction; (b) Surface plot of erosion rate vs. A × C interaction; (c) Surface plot of erosion rate vs. B × C interaction.*

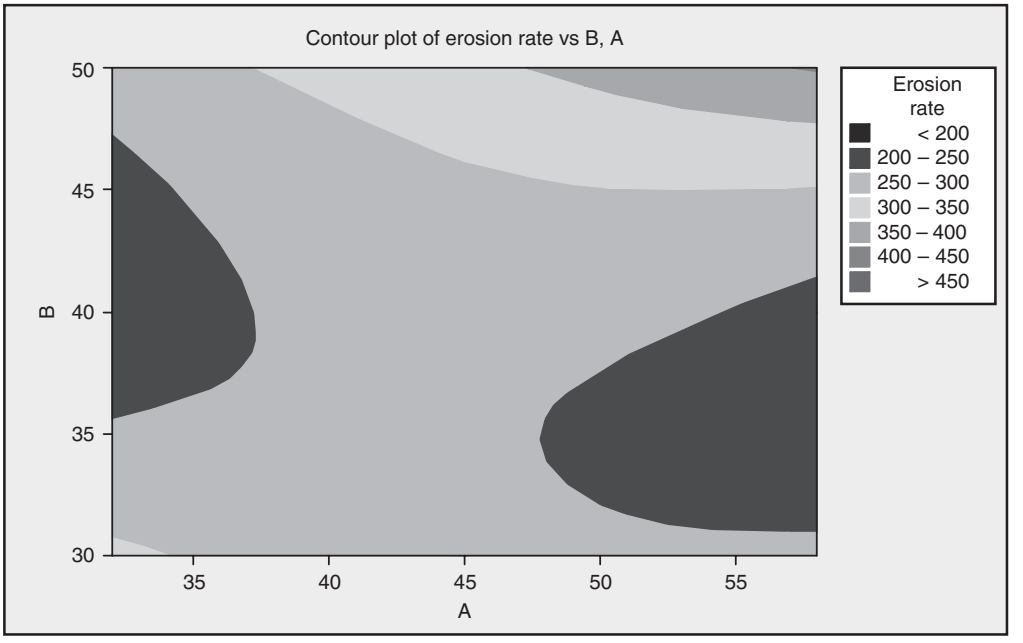

Figure 12. *Surface response plot.*

the crater without any fracture (and hence no erosion) will result in $\eta = 0$. In contrast, the material removal is, by ideal micro-cutting, $\eta = 1.0$ or 100%. If erosion occurs by lip or platelet formation and their fracture by repeated impact, as is usually the case in the case of ductile materials, the magnitude of η will be very low, i.e., $\eta \leq 100\%$. In the case of brittle materials, erosion occurs, usually by spalling and removal of large chunks of materials, resulting from the interlinking of lateral or radial cracks and thus η can be expected to be even greater than 100% [27]. The erosion efficiencies of the composites under the present study indicate that at low impact speed the erosion response is semi-ductile ($\eta = 10$–100%). On the other hand at relatively higher impact velocity, the composites exhibit ductile ($\eta < 10\%$) erosion behavior [28].

ANOVA and the Effects of Factors

In order to understand a concrete visualization of impact of various factors and their interactions, it is desirable to develop an analysis of variance (ANOVA) table to find out the order of significant factors as well as interactions. Table 5 shows the results of the ANOVA with the erosion rate. This analysis was undertaken for a level of confidence of significance of 5%. The last column of the table indicates that the main effects are highly significant (all have very small p-values).

From Table 5, one can observe that the fiber loading ($p = 0.004$), erodent size ($p = 0.145$), impingement angle ($p = 0.252$) and impact velocity ($p = 0.265$) have great influence on erosion rate. The interaction of impact velocity × fiber loading ($p = 0.029$) shows significance of contribution on the erosion rate and the factor stand-off distance ($p = 0.493$) and impact velocity × stand-off distance ($p = 0.150$), fiber loading × stand-off distance ($p = 0.162$) present less significance of contribution on erosion rate.

Table 4. Erosion efficiency of GF-reinforced polyester resin.

Sl. No.	Impact velocity (V) m/sec	Density of eroding material (ρ) kg/m^3	Hardness of eroding material (Hv) MPa	Erosion rate (Er) mg/kg	Erosion efficiency (η)
1	32	1738	32	309.83	43.70689
2	32	1738	32	315.25	12.83002
3	32	1738	32	305.19	10.76308
4	32	1874	34	186.07	7.462040
5	32	1874	34	272.79	9.479905
6	32	1874	34	230.96	32.10497
7	32	1932	39	287.69	11.12368
8	32	1932	39	279.85	43.28217
9	32	1932	39	255.25	11.38925
10	45	1738	32	288.86	5.944763
11	45	1738	32	249.80	4.454857
12	45	1738	32	255.25	18.20820
13	45	1874	34	239.76	4.213340
14	45	1874	34	249.18	17.51554
15	45	1874	34	298.23	6.047942
16	45	1932	39	261.17	20.42593
17	45	1932	39	364.31	8.220070
18	45	1932	39	389.94	7.624237
19	58	1738	32	315.10	3.382663
20	58	1738	32	245.19	10.52866
21	58	1738	32	219.89	2.724091
22	58	1874	34	261.27	11.05526
23	58	1874	34	239.76	2.926861
24	58	1874	34	210.66	2.228443
25	58	1932	39	369.47	5.018254
26	58	1932	39	452.81	5.329466
27	58	1932	39	391.45	18.42909

Table 5. ANOVA table for erosion rate.

Source	DF	Seq SS	Adj SS	Adj MS	*f*	*P*
A	2	2.3056	2.3056	1.1528	1.88	0.265
B	2	35.4646	35.4646	17.7323	28.95	0.004
C	2	1.0737	1.0737	0.5369	0.88	0.483
D	2	2.4297	2.4297	1.2149	1.98	0.252
E	2	3.9765	3.9765	1.9882	3.25	0.145
A∗B	4	21.5781	21.5781	5.3945	8.81	0.029
A∗C	4	7.5740	7.5740	1.8935	3.09	0.150
B∗C	4	7.1630	7.1630	1.7908	2.92	0.162
Error	4	2.4498	2.4498	0.6125		
Total	26	84.0150				

CONFIRMATION EXPERIMENT

The confirmation experiment is the final test in the design of experiment process. The purpose of the confirmation experiment is to validate the conclusions drawn during the analysis phase. The confirmation experiment is performed by conducting a new set of

Table 6. Results of the confirmation experiments for Erosion rate.

	Optimal control parameters	Prediction	Experimental
Level		**$A_2B_3D_2E_3$**	**$A_2B_3D_2E_3$**
S/N ratio for Erosion rate (db)		−50.8283	−49.5677

factor settings $A_2B_3D_2E_3$ to predict the erosion rate. The estimated S/N ratio for erosion rate can be calculated with the help of following prediction equation:

$$\hat{\eta}_1 = \bar{T} + (\bar{A}_2 - \bar{T}) + (\bar{B}_3 - \bar{T}) + [(\bar{A}_2\bar{B}_3 - \bar{T}) - (\bar{A}_2 - \bar{T}) - (\bar{B}_3 - \bar{T})] + (\bar{D}_2 - \bar{T}) + (\bar{E}_3 - \bar{T}) \tag{3}$$

where $\bar{\eta}_1$ is the predicted average, $\bar{T}$ is the overall experimental average and $\bar{A}_2$, $\bar{B}_3$, $\bar{D}_2$, and $\bar{E}_3$ are the mean responses for factors and interactions at designated levels.

By combining like terms, the equation reduces to

$$\bar{\eta}_1 = \bar{A}_2\bar{B}_3 + \bar{D}_2 + \bar{E}_3 - 2\bar{T}. \tag{4}$$

A new combination of factor levels A_2, B_3, D_2, and E_3 is used to predict deposition rate through prediction equation and it is found to be $\bar{\eta}_1 = -50.8283\,dB$. For each performance measure, an experiment was conducted for a different factor combination and compared with the result obtained from the predictive equation as shown in Table 6.

The resulting model seems to be capable of predicting erosion rate to a reasonable accuracy. An error of 2.48% for the S/N ratio of erosion rate is observed. However, the error can be further reduced if the number of measurements is increased. This validates the development of the mathematical model for predicting the measures of performance based on knowledge of the input parameters.

FACTOR SETTINGS FOR MINIMUM EROSION RATE

In this study, an attempt is made to derive optimal settings of the control factors for minimization of erosion rate. The single-objective optimization requires quantitative determination of the relationship between erosion rates with combination of control factors. In order to express the erosion rate in terms of a mathematical model, the following form is suggested:

$$Er = K_0 + K_1 \times A + K_2 \times B + K_3 \times D + K_4 \times E + K_5 \times A \times B. \tag{5}$$

Here, Er is the performance output term and K_i ($i = 0, 1, \ldots 5$) are the model constants. The constants are calculated using non-linear regression analysis with the help of SYSTAT 7 software and the following relations are obtained:

$$\begin{aligned} E_r &= 1.521 - 1.633A - 1.387B + 0.088D + 0.078E + 1.221AB \\ r^2 &= 0.98. \end{aligned} \tag{6}$$

The correctness of the calculated constants is confirmed as high correlation coefficients (r^2) in the tune of 0.98, obtained for Equation (6) and therefore, the models are quite

suitable to use for further analysis. Here, the resultant objective function to be maximized is given as:

$$\text{Maximize } Z = \frac{1}{f} \tag{7}$$

where, f is the normalized function for erosion rate.

Subjected to constraints:

$$A_{\min} < A < A_{\max} \tag{8}$$

$$B_{\min} < B < B_{\max} \tag{9}$$

$$D_{\min} < D < D_{\max} \tag{10}$$

$$E_{\min} < E < E_{\max}. \tag{11}$$

The min and max in Equations 8–11 shows the lowest and highest control factors settings (control factors) used in this study (Table 1).

Genetic algorithm (GA) is used to obtain the optimum value for single-objective outputs to optimize the single-objective function. This technique has been successfully implemented earlier for determining the optimal factor setting in the case of erosion wear of flyash filled glass-polyester composites [29]. The computational algorithm is implemented in Turbo C^{++} and run on an IBM Pentium IV machine. Genetic algorithms (GAs) are mathematical optimization techniques that simulate a natural evolution process. They are based on the Darwinian Theory, in which the fittest species survive and propagate while the less successful tend to disappear. Genetic algorithm mainly depends on three types of operators viz., reproduction, crossover and mutation. Reproduction is accomplished by copying the best individuals from one generation to the next, what is often called an elitist strategy. The best solution is monotonically improving from one generation to the next. The selected parents are submitted to the crossover operator to produce one or two children. The crossover is carried out with an assigned probability, which is generally rather high. If a randomly sampled number is inferior to the probability, the crossover is performed. The genetic mutation introduces diversity in the population by an occasional random replacement of the individuals. The mutation is performed based on an assigned probability. A random number is used to determine if a new individual will be produced to substitute the one generated by crossover. The mutation procedure consists of replacing one of the decision variable values of an individual while keeping the remaining variables unchanged. The replaced variable is randomly chosen and its new value is calculated by randomly sampling within its specific range. In genetic optimization, population size, probability of crossover and mutation are set at 50, 75, and 5% respectively for all the cases. The number of generation is varied till the output is converted. Table 7 shows the optimum conditions of the control factors with optimum performance output gives a better combination of set of input control factors.

CONCLUSIONS

This analytical and experimental investigation into the erosion behavior of glass fiber reinforced polyester composites leads to the following conclusions:

1. Solid particle erosion characteristics of these composites can be successfully analyzed using the Taguchi experimental design scheme. Taguchi method provides a simple,

Table 7. Optimum conditions for performance output.

Control factors and performance characteristics	Optimum conditions
A: Impact velocity (m/sec)	33.15
B: Fiber loading (%)	41.02
D: Impingement angle (degree)	59.45
E: Erodent size (μm)	500.0
Erosion rate (mg/kg)	364.72

systematic and efficient methodology for the optimization of the control factors. This approach, not only needs engineering judgment, but also requires a rigorous mathematical model to obtain optimal process settings.

2. The results indicate that erodent size, fiber loading, impingement angle and impact velocity are the significant factors in a declining sequence affecting the erosion wear rate. Although the effect of impact velocity is less compared with other factors, it cannot be ignored, because it shows significant interaction with fiber loading. An optimal parameter combination is determined, which leads to minimization of material loss due to erosion.
3. The composites exhibit semi-ductile erosion characteristics with the peak erosion wear occurring at a 60° impingement angle. This has been explained by analyzing the possible damage mechanism with the help of SEM micrographs. It is concluded that the inclusion of brittle fibers in ductile polyester matrix is responsible for this semi-ductility.
4. The erosion efficiency (η) values obtained experimentally also suggest that the glass fiber reinforced polyester composites exhibit semi-ductile erosion response ($\eta = 10$–60%) for low impact velocities. However, for relatively high impact velocity, they present a ductile erosion response ($\eta < 10\%$).
5. The rationale behind the use of genetic algorithm lies in the fact that genetic algorithm has the capability to find the global optimal parameter settings, whereas the traditional optimization techniques are normally stuck up at the local optimum values. The optimum settings are found to be impact velocity $= 33.15$ m/sec, fiber loading $= 41.02\%$, impingement angle $= 59.45^\circ$, erodent size $= 500.0\,\mu$m, and resulting erosion rate $= 364.72$ mg/kg, as far as present experimental conditions are concerned.
6. This work leaves wide scope for future investigators to study the erosion behavior of such composites with short fiber reinforcement and with particulate filling.

REFERENCES

1. Wahl, H. and Hartenstein, F. (1946). *Strahlverschleiss, Frankh'sche Verlagshandlung*, Stuttgart.
2. Bitter, J. G. A. (1963). A Study of Erosion Phenomena, Part II, *Wear*, **6**: 169–190.
3. Raask, E. (1969). Tube Erosion by Ash impaction, *Wear*, **13**: 301–315.
4. Hibbert, W. A. (1965). Helicopter trials over sand and sea, *J. Roy. Aero. Soc.*, **69**: 769–776.
5. Pool, K. V., Dharan, C. K. H. and Fimmie, I. (1986). Erosion Wear of Composite Materials, *Wear*, **107**: 1–12.
6. Kulkarni, S. M. and Kishore, K. (2001). Influence of Matrix Modification on the Solid Particle Erosion of Glass/Epoxy Composites, *Polym. Polym. Composites*, **9**: 25–30.
7. Aglan, H. A. and Chenock Jr, T. A. (1993). Erosion Damage Features of Polyimide Thermoset Composites, *SAMPEQ*, **24**(2): 41–47.
8. Barkoula, N. M. and Karger-Kocsis, J. (2002). Effect of Fiber Content and Relative Fiber-orientation on the Solid Particle Erosion of GF/PP Composite, *Wear*, **252**: 80–87.

9. Tewari, U. S., Harsha, A. P., Hager, A. M. and Friedrich, K. (2002). Solid Particle Erosion of Unidirectional Carbon Fiber Reinforced Polyetheretherketone Composites, *Wear*, **252**: 992–1000.
10. Häger, A., Friedrich, K., Dzenis, Y. A. and Paipetis, S. A. (1995). Study of Erosion Wear of Advanced Polymer Composites, In: K. Street, B.C. Whistler (Eds), *Proceedings of the ICCM-10*, Canada Wood head Publishing Ltd., Cambridge, 155–162,
11. Miyazaki, N. and Takeda, T. (1993). Solid Particle Erosion of Fiber Reinforced Plastic, *J. Compos. Mater.*, **27**: 21–31.
12. Tilly, G. P. and Sage, W. (1970). The Interaction of Particle and Material Behaviour in Erosion Process, *Wear*, **16**: 447–65.
13. Lindsley, B. A. and Marder, A. R. (1999). The Effect of Velocity on the Solid Particle Erosion Rate of Alloys, *Wear*, **225–229**: 510–516.
14. Sundararajan, G. and Roy, M. (1997). Solid Particle Erosion Behaviour of Metallic Materials at Room and Elevated Temperatures, *Tribology International*, **30**: 339–359.
15. Mahapatra, S. S. and Patnaik, A. (2006). Development and Analysis of Wear Resistance Model for Composites of Aluminium Reinforced with Redmud, *The Journal of Solid Waste Technology and Management*, **32**(1): 28–35.
16. Mahapatra, S. S. and Patnaik, A. (2006). Optimization of Parameter Combinations in Wire Electrical Discharge Machining using Taguchi Method, *Indian Journal of Engineering & Material Sciences*, **13**: 493–502.
17. Mahapatra, S. S. and Patnaik, A. (2006). Optimization of Wire Electrical Discharge Machining (WEDM) process Parameters using Genetic Algorithm, *Int. J. Adv. Manuf. Technol.* DOI.10.1007/s00170-006-0672-6.
18. Mahapatra, S. S. and Patnaik, A. (2007). Parametric Optimization of Wire Electrical Discharge Machining (WEDM) Process using Taguchi method, *Journal of the Brazilian Society of Mechanical Sciences,* **28**(4): 423–430.
19. Mahapatra, S. S. and Patnaik, A. (2006). Determination of Optimal Parameter settings in Wire Electrical Discharge Machining (WEDM) Process using Taguchi method, *The Institution of Engineering*, **87**: 16–24.
20. Mahapatra, S. S. and Patnaik, A. (2006). Parametric Analysis and Optimization of Drilling of Metal Matrix Composites based on the Taguchi Method, *The International Journal for Manufacturing Science and Technology*, **8**(1): 5–12.
21. Mahapatra, S. S. and Patnaik, A. (2007).Optimization of Wire Electrical Discharge Machining (WEDM) Process Parameters using Taguchi method, *The International Journal for Manufacturing Science and Technology*, **9**(2): 129–136.
22. Glen, S. P. (1993). *Taguchi Methods: A Hands on Approach*, Addison-Wesley, New York.
23. Phadke, M. S. (1989). *Quality Engineering using Robust Design*, Prentice Hall, Eaglewood Cliffs, New Jersey.
24. Sundararajan, G., Roy, M. and Venkataraman, B. (1990). Erosion Efficiency – A New Parameter to Characterize the Dominant Erosion Micromechanism, *Wear*, **140**: 369–381.
25. Hutchings, I. M., Winter, R. E. and Field, J. E. (1976). Solid Particle Erosion of Metals: the Removal of Surface Material by Spherical Profectiles, *Proc. Roy. Soc. Lond., Ser.* A **348**: 379–392.
26. Srivastava, V. K. and Pawar, A. G. (2006). Solid Particle Erosion of Glass Fiber Reinforced Flyash Filled Epoxy Resin Composites, *Composite Science and Technology*, **66**: 3021–3028.
27. Arjula, S. and Harsha, A. P. (2006). Study of Erosion Efficiency of Polymers and Polymer Composites, *Polymer Testing,* **25**: 188–196.
28. Roy, M., Vishwanathan, B. and Sundararajan, G. (1994). The Solid Particle Erosion of Polymer Matrix Composites, *Wear*, **171**: 149–161.
29. Patnaik, A., Satapathy, A. Mahapatra, S. S. and Dash, R. R. (2007). Modeling and Prediction of Erosion Response of Glass Reinforced Polyester-Flyash Composites, *Journal of Reinforced Plastics and Composites* (in press).